

Boosting Segment Anything Model Towards Open-Vocabulary Learning

Xumeng Han^{1*} Longhui Wei² Xuehui Yu¹ Zhiyang Dou¹ Xin He²
Kuiran Wang¹ Zhenjun Han^{1†} Qi Tian^{2†}

¹ University of Chinese Academic of Sciences ² Huawei Cloud

<https://github.com/ucas-vg/Sambor>

Abstract

The recent Segment Anything Model (SAM) has emerged as a new paradigmatic vision foundation model, showing potent zero-shot generalization and flexible prompting. Despite SAM finding applications and adaptations in various domains, its primary limitation lies in the inability to grasp object semantics. In this paper, we present **Sambor** to seamlessly integrate SAM with the open-vocabulary object detector in an end-to-end framework. While retaining all the remarkable capabilities inherent to SAM, we enhance it with the capacity to detect arbitrary objects based on human inputs like category names or reference expressions. To accomplish this, we introduce a novel SideFormer module that extracts SAM features to facilitate zero-shot object localization and inject comprehensive semantic information for open-vocabulary recognition. In addition, we devise an open-set region proposal network (Open-set RPN), enabling the detector to acquire the open-set proposals generated by SAM. Sambor demonstrates superior zero-shot performance across benchmarks, including COCO and LVIS, proving highly competitive against previous SoTA methods. We aspire for this work to serve as a meaningful endeavor in endowing SAM to recognize diverse object categories and advancing open-vocabulary learning with the support of vision foundation models.

1. Introduction

Vision foundation models [18, 25, 36, 38] serve as robust backbones that excel across a diverse spectrum of vision tasks. The recent *Segment Anything Model* (SAM) [25] has garnered widespread attention within the community as a foundational visual model for general image segmentation. Trained with billion-scale mask labels, it demonstrates impressive zero-shot segmentation performance, seamlessly applied across a variety of applications through simple

*This work was done when X. Han (hanxumeng19@mails.ucas.ac.cn) was an intern at Huawei Cloud.

†Corresponding author: hanzhj@ucas.ac.cn, tian.qi1@huawei.com.

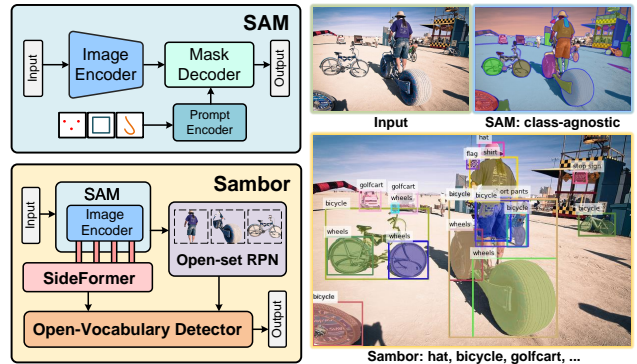


Figure 1. We construct an end-to-end open-vocabulary object detector named **Sambor**, building upon the vision foundation model SAM. Sambor endows SAM with the ability to recognize arbitrary object categories, effectively addressing semantic gaps. On the other hand, Sambor draws upon the powerful generalization and rich interactive functionalities embedded in SAM, improving the zero-shot performance and extending the versatility of the open-vocabulary object detector.

prompting [1, 47]. While exhibiting outstanding performance, SAM is constrained to scenarios with class-agnostic applications, necessitating a more profound exploration to enhance its semantic understanding. In this work, we boost SAM towards open-vocabulary learning to detect objects of arbitrary categories, a paradigm commonly referred to as *open-vocabulary object detection*.

Recent works [10, 14, 27, 28, 32, 35, 52, 62] commonly follow two lines to achieve open-vocabulary object detection. One seeks to expand the cognitive categories by transferring knowledge from pre-trained vision-language (VL) models [20, 38]. The other unifies the formulation of object detection and phrase grounding tasks, extending the available data scope from object detection to a diverse range of image-text pairs [41, 44, 46]. The utilization of large-scale data encourages the model to learn the feature alignment between object regions and language phrases. Previous efforts have been built upon conventional object detection models, introducing the VL paradigm to extend the object detection classifier from close-set to open-set domain. With the emer-

gence of the powerful vision foundation model SAM, its remarkable zero-shot localization capabilities and the flexibility for interactive prompting raise the prospect of elevating open-vocabulary object detection to new heights.

In this paper, we introduce *Sambor* (which stands for *SAM BOosteR*), as illustrated in Fig. 1. Sambor is an end-to-end open-vocabulary object detection framework that seamlessly integrates all functionalities from the SAM, inheriting its powerful zero-shot generalization and flexible prompting. We establish a ladder side transformer adapter, named SideFormer, on the frozen SAM image encoder. Primarily, it incorporates an extractor designed to integrate features from the image encoder, aiming to harness the zero-shot object-aware capabilities of SAM features, providing assistance in open-set object localization. Subsequently, we devise an injector within SideFormer to augment the original features by introducing additional semantic information. In pursuit of the injected features imbued with rich semantics, CLIP [38], another vision foundation model, naturally emerges as our excellent choice, given its outstanding zero-shot classification capabilities through VL alignment. As a result, infusing CLIP visual features not only enhances semantic understanding but also narrows the gap with the text feature domain, providing convenience for the open vocabulary object classifier [14, 27].

Moreover, SAM exhibits the capacity to generate high-quality class-agnostic proposals. To fully leverage this advantage and further augment the zero-shot localization ability, we develop the open-set region proposal network (Open-set RPN). Specifically, Sambor adopts the two-stage object detection architecture, decoupling the detector into a first stage dedicated to generating high-quality proposals to ensure sufficient recall, and a second stage focused on open-vocabulary classification. Open-set RPN complements the vanilla RPN [39] by introducing proposals oriented towards open-set scenarios. Thanks to the flexibility afforded by SAM, these additional proposals can be obtained through various prompts or the automatic mask generation pipeline.

We follow the GLIP [28] protocol and conduct experiments to comprehensively evaluate the effectiveness of Sambor in open-vocabulary object detection. Benefiting from the effective designs, Sambor demonstrates superior open-vocabulary detection performance on COCO [31] and LVIS [15] benchmarks. It implies that we endow SAM with the capability to recognize arbitrary objects, boosting it to be more versatile. From another perspective, incorporating SAM into an end-to-end framework provides greater versatility compared to current state-of-the-art open-vocabulary detectors. For instance, it allows for seamless conversion of object detection results into instance segmentation or facilitates human-machine interaction through prompts. These capabilities are previously either unavailable or required the cascading of multiple models [1], introducing additional

complexity and operational challenges. Given these encouraging results, we aspire to endow the vision foundation model SAM with recognition capabilities to address a broader spectrum of applications and offer a potential way for the development of open-vocabulary object detection.

2. Related Work

Segment Anything Model [25] is an innovative image segmentation model, trained on the dataset comprising over 1 billion masks. It aims to robustly segment any object guided by diverse prompts. HQ-SAM [22] extends SAM with a learnable high-quality output token which proves efficient in diverse segmentation domains. SAM-Adapter propose the adaptation approach. In addition, X-Decoder [67] proposes a generic decoder that can handle complex visual tasks such as open-vocabulary panoptic segmentation without fine-tuning. SEEM [68] introduces an interactive model that supports multi-modal prompt inputs like scribbles and boxes to deal with the task of segmenting everything. OpenSeeD [58] is the first work to combine detection data and segmentation data for joint training in the open-vocabulary segmentation task.

Open-Vocabulary Object Detection [14, 27, 28, 32, 35, 50, 53–55, 65] aims to detect objects of unbounded concepts using a more universal and practical paradigm. For instances, [10, 14, 62] leverage vision-language model (VLM) [20, 38] to align information between regions and words through a multi-stage pre-training strategy. CORA [49] effectively narrows the gap between global and regional features by incorporating visual cues. CoDet [34] implicitly leverages the correspondences of regions to bridge regions and words. BARON [48] aligns bag of regions with words, making better use of structured semantic information. GLIP [28] pioneers an alternative approach that transforms the detection data into a grounding format and introduces a fusion module for simultaneous learning of vision-language alignment and object localization. Det-CLIP [52] integrates detection, grounding, and image-text pair data in a parallel framework and creates a concept dictionary to enhance the text data. Compared to previous methods, we leverage the localization capabilities of SAM to alleviate the limited awareness of the intricate alignment between regions and words in VLM, presenting a novel and potentially effective solution.

Parameter-Efficient Transfer Learning. The paradigm of fine-tuning pre-trained models on downstream tasks has witnessed a shift from traditional comprehensive parameter adjustments towards more parameter-efficient techniques. Adapters [11, 43, 60] integrates trainable modules within a fixed model architecture; prompt-based methods [23, 51, 63, 64] fine-tune prompts for text, images, or both modalities, respectively. [6, 42, 59] employs an ad-

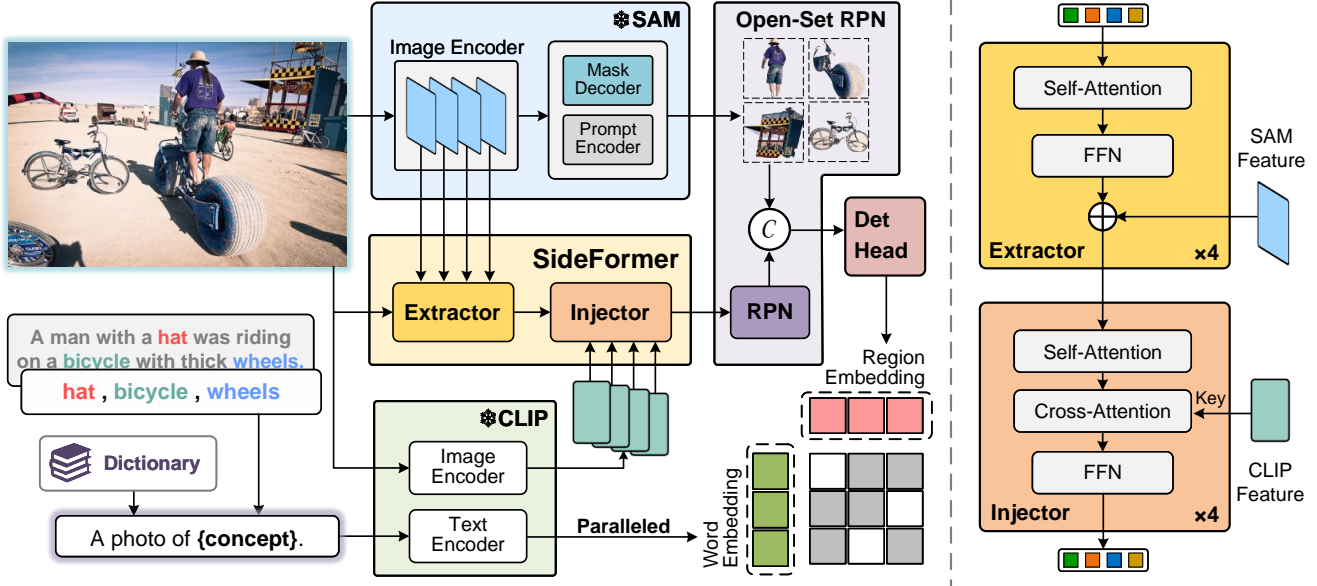


Figure 2. **Overall architecture of Sambor.** (Left) We construct a SideFormer to extract features from SAM and inject CLIP visual features for enhancing semantic understanding. Building upon a two-stage detector, we devise an Open-set RPN that augments the vanilla RPN with open-set proposals generated by SAM. The language branch of CLIP encodes concepts in parallel, thereby empowering the detector with open-vocabulary recognition. (Right) The specific implementations of the extractor and injector in SideFormer.

ditive approach with a side network that merges its output with that of the backbone of the visual foundation model. In conceptual similarity with [6, 42], we build a side adapter module, named SideFormer, to efficiently transfer the localization ability of SAM and inject the semantic information from CLIP features for open-vocabulary recognition.

3. Methodology

3.1. Overall Architecture

An overview framework of the proposed approach is illustrated in Fig. 2, comprising four components as follows.

SAM [25] is composed of three modules: (1) Image encoder: a robust ViT-based backbone excels at extracting features from high-resolution images. (2) Prompt encoder: encoding the interactive positional information from the input points, boxes, or masks to provide for the mask decoder. (3) Mask decoder: a lightweight transformer-based decoder efficiently translates the image embedding, prompt embeddings, and an output token into a mask.

We employ the SAM image encoder as the backbone of Sambor and maintain parameter freeze during training. The SAM head, comprising the prompt encoder and the mask decoder, is utilized to generate open-set region proposals and transform detected open-vocabulary objects into instance segmentation results.

CLIP [38] leverages web-scale image-text pairs crawled from the Internet and simply aligning image features with

text features via contrastive learning, delivering impressive results in zero-shot image classification. We employ the CLIP visual encoder to extract semantic information, complementing the SAM encoder, and the CLIP text encoder supplants the conventional classifier in the object detector. In this paper, we choose the CNN-based CLIP model (e.g., RN50×64 [16]) over the ViT-based [9] one due to its superior compatibility with high-resolution image inputs [27].

SideFormer. Due to the absence of a semantic prior in the SAM feature encoder, its performance in category-aware tasks falls short of optimal. To address this issue, we introduce a ladder side transformer adapter SideFormer. This integration infuses more comprehensive semantic context without compromising the integrity of the original features.

SideFormer consists of an extractor for acquiring SAM features that excel in precise object localization. Additionally, it incorporates an injector custom-tailored for assimilating CLIP features, thereby enhancing semantic comprehension. More details are elaborated in Sec. 3.2.

Open-vocabulary object detector. Sambor is constructed on the two-stage object detector Cascade R-CNN [3] (following the ViTDet [29] architecture) and equipped with a text encoder for open-vocabulary classification. In our design, text embeddings are solely utilized to predict word-region similarity scores without the additional cross-modal fusion adopted in [28, 32]. Additionally, given the scarcity of segmentation annotations in most datasets, we have omitted the mask prediction head [17] in the detector to accom-

moderate training on diverse datasets. Thanks to the seamless integration of the complete SAM within our architecture, Sambor can effortlessly feed the detection results back to the SAM head, thereby achieving instance segmentation.

Furthermore, we extend the Region Proposal Network (RPN) [39] from the first stage into an Open-set RPN by incorporating more region proposals from the SAM head. We provide a detailed exposition in Sec. 3.3.

3.2. SideFormer

SAM extractor. We employ the patch embedding layer [9] with a structure identical to SAM [25] (without parameter sharing) to initially project the input image into visual tokens. The visual tokens are first summed with those from SAM, and then incrementally fused with the deeper SAM features via a series of transformer layers [45]. Following the ViTDet [29] architecture, SAM divides the ViT [9] backbone into four blocks, applying global attention at the last layer in each block. In view of this, we design *four* corresponding transformer layers to extract features from each global attention outputs.

For each transformer layer, the input visual tokens $\mathcal{F}_{\text{side}} \in \mathbb{R}^{\frac{HW}{16^2} \times D}$, where HW represents the input image size and D is the feature dimension, are encoded through a self-attention layer and a feed-forward network (FFN). Subsequently, we employ a direct summation to accomplish the fusion with the extracted SAM features $\mathcal{F}_{\text{sam}} \in \mathbb{R}^{\frac{HW}{16^2} \times D}$. This process can be formulated as:

$$\hat{\mathcal{F}}_{\text{side}} = \mathcal{F}_{\text{side}} + \text{Attn}(\text{norm}(\mathcal{F}_{\text{side}})), \quad (1)$$

$$\mathcal{F}'_{\text{side}} = \mathcal{F}_{\text{sam}} + \gamma \cdot (\hat{\mathcal{F}}_{\text{side}} + \text{FFN}(\text{norm}(\hat{\mathcal{F}}_{\text{side}}))), \quad (2)$$

where $\text{norm}(\cdot)$ is LayerNorm [2]. In addition, we apply a learnable vector $\gamma \in \mathbb{R}^D$ to modulate the transformer output, which is initialized with $\mathbf{0}$. This initialization strategy guarantees that the feature distribution of SideFormer commences from SAM without undergoing drastic alterations.

CLIP injector. After integrating features extracted from SAM, we imbue them with semantically rich information from the CLIP [38] visual encoder. The injector is also equipped with *four* transformer layers, supplemented by a cross-attention module for feature interaction.

We treat the input feature $\mathcal{F}'_{\text{side}}$ as the query, and the CLIP feature $\mathcal{F}_{\text{clip}}$ as the key and value. Initiate a self-attention encoding on the query first. Subsequently, we employ cross-attention on queries $\mathcal{F}'_{\text{side}}$ and $\mathcal{F}_{\text{clip}}$, facilitating the assimilation of knowledge from CLIP. Finally, a FFN is appended, constituting the entirety of this transformer layer. Eq. 3 details the cross-attention module in the injector, while omitting the self-attention and FFN for brevity.

$$\mathcal{F}^*_{\text{side}} = \mathcal{F}'_{\text{side}} + \gamma \cdot \text{Attn}(\text{norm}(\mathcal{F}'_{\text{side}}), \text{norm}(\mathcal{F}_{\text{clip}})), \quad (3)$$

where the learnable parameter γ is introduced to likewise balance the injected CLIP features with the original inputs.

3.3. Open-Set RPN

For a two-stage object detector, *e.g.*, Cascade R-CNN [3] adopted in this paper, the first stage involves the RPN [39] for generating class-agnostic region proposals. The second stage refines the positions of these proposals and predicts their respective categories. The detection performance heavily relies on the RPN recall. Hence, for the open-vocabulary object detector, possessing a robust RPN tailored for open-set domains is imperative.

For our Sambor, in addition to a trainable RPN, the integrated SAM head inherently serves as a class-agnostic mask proposal generator, showcasing robust zero-shot localization abilities. Consequently, the proposals generated by the SAM head serve as a valuable complement to the results from RPN. Specifically, we leverage the automatic mask generation pipeline [25], and extract bounding boxes from the resulting masks as region proposals. We employ the straightforward post-processing approach, *i.e.*, Non-Maximum Suppression (NMS), to merge two sets of region proposals. We retain all proposals from the RPN and subsequently filter out redundancies based on them. Proposals with a high Intersection over Union (IoU), using a default threshold of 0.7, are excluded, while the remaining suggestions are preserved as supplements. Further experimental details are available in Sec. 4.3.2. The automatic mask generation employs a regular grid of points as prompts, predicting a set of mask proposals for each point. Adjusting the density of these points manually allows for flexible control over proposal quantity. Unless otherwise specified, we default to a 32×32 grid of points in this paper as a trade-off between proposal quantity and computational cost.

3.4. Open-Vocabulary Object Detection

As illustrated in Fig. 2, the integrated features via SideFormer are fed into the object detector, generating a set of bounding boxes $B = \{\mathbf{b}_k\}_{k=1}^K$ (K is the number of predictions) along with the corresponding classification features $\mathcal{F}^B \in \mathbb{R}^{K \times D}$. Further, in order to expand the object recognition into the open-vocabulary domain, we introduce a language branch, *i.e.*, the CLIP [38] text encoder. We insert each concept name into the prompt template (*e.g.*, 'A photo of {concept}.') to form a complete sentence. These sentences are separately forwarded to the text encoder for obtaining sentence embeddings $\mathcal{F}^T \in \mathbb{R}^{M \times D}$, where M is the number of concepts sampled in each batch. We calculate the similarity matrix $S = \mathcal{F}^B \cdot (\mathcal{F}^T)^\top \in \mathbb{R}^{K \times M}$ to construct the word-region alignment loss [28].

Unified data formulation. Following [52, 53], we employ a *paralleled* formulation to unify the data formats from object detection and phrase grounding.

- **Object detection.** A concept set is derived from the names of all the categories in the dataset. Categories

| Method | Backbone | #Trainable Params | Pre-Train Data | Data Size | COCO 2017val | | | | | |
|---------------------------------|------------------------|-------------------|---------------------|-----------|-----------------|-------------------------------|-------------------------------|-----------------|-------------------------------|-------------------------------|
| | | | | | AP ^b | AP ₅₀ ^b | AP ₇₅ ^b | AP ^m | AP ₅₀ ^m | AP ₇₅ ^m |
| DyHead-T [†] [7] | Swin-T [33] | ≈100M | - | - | 49.7 | 68.0 | 54.3 | - | - | - |
| DINO (Swin-L) [†] [56] | Swin-L [33] | 218M | - | - | 58.5 | 77.0 | 64.0 | - | - | - |
| ViTDet [†] [29] | ViT-B [9] | 141M | - | - | 54.0 | 72.2 | 58.9 | 46.7 | 69.8 | 50.9 |
| DyHead-T [7] | Swin-T [33] | ≈100M | O365 | 0.66M | 43.6 | - | - | - | - | - |
| GLIP-T (B) [28] | Swin-T [33] | 232M | O365 | 0.66M | 44.9 | 61.5 | 49.0 | - | - | - |
| GLIP-T (C) [28] | Swin-T [33] | 232M | O365,GoldG | 1.46M | 46.7 | 63.4 | 51.1 | - | - | - |
| GLIP-T [28] | Swin-T [33] | 232M | O365,GoldG,CC3M,SBU | 5.46M | 46.6 | 63.1 | 50.8 | - | - | - |
| DINO (Swin-T) [56] | Swin-T [33] | 49M | O365 | 0.66M | 46.2 | - | - | - | - | - |
| Grounding-DINO-T [32] | Swin-T [33] | 172M | O365 | 0.66M | 46.7 | - | - | - | - | - |
| Grounding-DINO-T [32] | Swin-T [33] | 172M | O365,GoldG | 1.46M | 48.1 | - | - | - | - | - |
| Grounding-DINO-T [32] | Swin-T [33] | 172M | O365,GoldG,Cap4M | 5.46M | 48.4 | 64.4 | 53.0 | - | - | - |
| Sambor (Ours) | ViT-B [‡] [9] | 160M | O365 | 0.66M | 47.3 | 64.7 | 51.3 | 36.5 | 59.8 | 38.3 |
| Sambor [★] (Ours) | ViT-B [‡] [9] | 160M | O365 | 0.66M | 48.6 | 66.1 | 52.7 | 37.1 | 60.6 | 38.8 |

Table 1. **Zero-shot performance** on COCO benchmark. AP^b and AP^m indicate the AP values for object detection (bounding boxes) and instance segmentation (masks), respectively. [★] denotes the application of Open-set RPN. [†] denotes supervised approaches. [‡] denotes that the parameters in backbone are frozen.

present in the image are considered positives, while those absent are treated as negative concepts. Since the category names in the object detection dataset remain constant, pre-extracting and storing all category features before training proves advantageous. It eliminates the need for repetitive feature extraction in each iteration, thereby enhancing training efficiency. In addition, for each category, the average of all provided prompt templates is computed to serve as its feature. This policy is equally applicable during the inference phase.

- **Phrase grounding.** We extract phrases corresponding to labeled objects from the original caption, forming a positive concept set. To offer diverse negatives similar to the object detection data, we assemble a negative concept set for learning purposes. Opting for the off-the-shelf mega-scale and information-dense Bamboo [61] dataset, we filter out a subset of entity concepts to serve as the negative concept set. For phrase grounding data, handling text features offline is unfeasible due to the variability in concept names in images across different iterations. Consequently, for each batch, we draw a subset of concepts from the pool to serve as negatives, with the default setting the total number of positive and negative concepts to 150. Additionally, for time efficiency, we randomly select a prompt template to extract text features.

4. Experiments

4.1. Implementation Details

Training dataset. For object detection data, we use the Objects365 [40] dataset (referred to as O365), which contains 0.66M images across 365 categories. In terms of

phrase grounding data, we employed GoldG [21], comprising 0.8M human-annotated instances from sources including Flickr30K [37], VG Caption [26], and GQA [19]. We deliberately excluded COCO [31] images to ensure a more equitable evaluation of zero-shot performance.

Training details. We pre-train our models using SAM [25] with ViT-B [9] as the backbone and CLIP [38] with RN50×64 [16], utilizing 16 GPUs with a batch size of 64. We select AdamW [24] optimizer with a 0.05 weight decay, an initial learning rate 4×10^{-4} and a cosine annealing learning rate decay. The default training schedule is 12 epochs. We exclusively train the SideFormer and detection head, while keeping the other parameters frozen. The input image size is $1,024 \times 1,024$ with standard scale jittering [12]. This size is uniformly employed as the input for SAM, CLIP and SideFormer modules. The max token length for each input sentence follows the CLIP default setting of 77. MMDetection [4] code-base is used.

4.2. Zero-Shot Performance

COCO benchmark. COCO [31], comprising 80 common object categories, stands as the most widely utilized dataset in the field of object detection. Considering that O365 has covered all 80 common categories in COCO and is frequently employed as pre-training data for COCO, we focus on evaluating the zero-shot transfer performance for models pre-trained with O365 on the COCO benchmark.

We provide a comparison between GLIP [28] and Grounding DINO [32], along with their underlying object detectors (DyHead and DINO) in Table 1. Sambor outperforms all previous models on the zero-shot transfer settings. When trained on the same O365 dataset, Sambor shows

| Method | Backbone | #Trainable Params | Pre-Train Data | Data Size | MiniVal [21] | | | | Val v1.0 | | | |
|------------------------------|------------------------|-------------------|-------------------|-----------|--------------|-----------------|-----------------|-----------------|-------------|-----------------|-----------------|-----------------|
| | | | | | AP | AP _r | AP _c | AP _f | AP | AP _r | AP _c | AP _f |
| MDETR [†] [21] | RN101 [16] | 186M | GoldG+,RefC | 0.9M | 24.2 | 20.9 | 24.9 | 24.3 | - | - | - | - |
| Mask R-CNN [†] [21] | RN101 [16] | 69M | - | - | 33.3 | 26.3 | 34.0 | 33.9 | - | - | - | - |
| GLIP-T (B) [28] | Swin-T [33] | 232M | O365 | 0.66M | 17.8 | 13.5 | 12.8 | 22.2 | 11.3 | 4.2 | 7.6 | 18.6 |
| GLIP-T (C) [28] | Swin-T [33] | 232M | O365,GoldG | 1.46M | 24.9 | 17.7 | 19.5 | 31.0 | 16.5 | 7.5 | 11.6 | 26.1 |
| GLIP-T [28] | Swin-T [33] | 232M | O365,GoldG,Cap4M | 5.46M | 26.0 | 20.8 | 21.4 | 31.0 | 17.2 | 10.1 | 12.5 | 25.5 |
| GLIPv2-T [57] | Swin-T [33] | 232M | O365,GoldG,Cap4M | 5.46M | 29.0 | - | - | - | - | - | - | - |
| DetCLIP-T (A) [52] | Swin-T [33] | - | O365 | 0.66M | 28.8 | 26.0 | 28.0 | 30.0 | 22.1 | 18.4 | 20.1 | 26.0 |
| DetCLIP-T (B) [52] | Swin-T [33] | - | O365,GoldG | 1.46M | 34.4 | 26.9 | 33.9 | 36.3 | 27.2 | 21.9 | 25.5 | 31.5 |
| DetCLIP-T [52] | Swin-T [33] | - | O365,GoldG,YFCC1M | 2.46M | 35.9 | 33.2 | 35.7 | 36.4 | 28.4 | 25.0 | 27.0 | 31.6 |
| DetCLIPv2-T [53] | Swin-T [33] | - | O365 | 0.66M | 28.6 | 24.2 | 27.1 | 30.6 | - | - | - | - |
| DetCLIPv2-T [53] | Swin-T [33] | - | O365,CC3M | 3.66M | 31.3 | 29.4 | 31.7 | 31.3 | - | - | - | - |
| DetCLIPv2-T [53] | Swin-T [33] | - | O365,GoldG,CC3M | 4.46M | 38.4 | 36.7 | 37.9 | 39.1 | - | - | - | - |
| Grounding-DINO-T [32] | Swin-T [33] | 172M | O365,GoldG | 1.46M | 25.6 | 14.4 | 19.6 | 32.2 | - | - | - | - |
| Grounding-DINO-T [32] | Swin-T [33] | 172M | O365,GoldG,Cap4M | 5.46M | 27.4 | 18.1 | 23.3 | 32.7 | - | - | - | - |
| Sambor (Ours) | ViT-B [‡] [9] | 160M | O365 | 0.66M | 32.7 | 29.5 | 32.1 | 33.9 | 26.2 | 22.7 | 24.0 | 30.2 |
| Sambor [★] (Ours) | ViT-B [‡] [9] | 160M | O365 | 0.66M | 33.1 | 29.6 | 32.0 | 34.7 | 26.3 | 20.9 | 24.4 | 30.9 |
| Sambor [★] (Ours) | ViT-B [‡] [9] | 160M | O365,GoldG | 1.46M | 39.6 | 34.6 | 39.3 | 40.7 | 32.8 | 30.9 | 31.0 | 35.7 |

Table 2. **Zero-shot performance** on LVIS benchmark. *Fixed AP* [8] is reported. AP_r, AP_c, and AP_f indicate the AP values for rare, common and frequent categories, respectively. [★] denotes the application of Open-set RPN. [†] denotes supervised approaches. [‡] denotes that the parameters in backbone are frozen.

+**2.4** AP and +**0.6** AP compared to GLIP and Grounding DINO, respectively. When employing the Open-set RPN (see more details in Sec. 4.3.2), Sambor demonstrates the best performance, surpassing even models that utilize a larger dataset. We additionally report the zero-shot instance segmentation performance, which is effortlessly achievable by feeding the detection outputs into the SAM head. Notably, in comparison to other models, Sambor has a lower count of trainable parameters. This is attributed to the fact that, aside from SideFormer and the detection head, all parameters of the remaining components are frozen.

LVIS benchmark. LVIS [15] contains 1,203 categories, including numerous rare categories that are seldom encountered in pre-training datasets. We report the *Fixed AP* [8] on both the MiniVal [21] subset, comprising 5,000 images, and the complete validation set v1.0.

The zero-shot performance on the LVIS benchmark is presented in Table 2. Here, we also report the performance with and without the use of Open-set RPN, revealing an improvement of 0.4 AP when employed. Under comparable volumes of training data, Sambor outperforms competitors by a large margin. Specifically, in the scenario of training solely on O365 and evaluating on LVIS MiniVal, our model outperforms GLIP by **15.3** AP, and surpasses DetCLIP / DetCLIPv2 by **4.3** / **4.5** AP, respectively. The advantage is similarly pronounced when compared to Grounding DINO. Furthermore, we incorporate the phrase grounding

dataset GoldG to enhance the generalization ability of Sambor. To improve efficiency, instead of training from scratch, we fine-tune the O365 pre-trained model for 3 epochs while keeping all other settings consistent. Remarkably, Sambor exhibits significantly enhanced zero-shot performance across all categories, surpassing even the results achieved by other methods utilizing larger datasets.

4.3. Ablation Studies

We conduct a series of ablation studies on Sambor. Unless specified otherwise, training is performed on the O365 dataset using default settings.

4.3.1 Effectiveness of SideFormer

We propose the SideFormer, as described in Sec. 3.2, to amalgamate features from SAM and CLIP, improving the capacity for object localization and recognition. Table 3 verifies the effect of our design on both COCO and LVIS datasets. The Sambor baseline denotes the direct connection of the deepest features from the SAM backbone to the Cascade R-CNN [3] detector. The incorporation of the SAM feature extractor consistently leads to improved performance. However, the model’s recognition abilities are still insufficient. To alleviate this, we introduce the CLIP feature injector to enhance the semantic representation, thereby achieving the best performance. Furthermore, as we utilize CLIP text features for classification, a clear

| Strategy | COCO val | | | LVIS MiniVal | | | |
|-----------------|-------------|------------------|------------------|--------------|-----------------|-----------------|-----------------|
| | AP | AP ₅₀ | AP ₇₅ | AP | AP _r | AP _c | AP _f |
| Sambor baseline | 39.0 | 54.7 | 42.5 | 27.7 | 21.5 | 26.5 | 29.9 |
| + SAM Extractor | 42.4 | 58.7 | 46.2 | 29.0 | 25.2 | 27.5 | 31.0 |
| + CLIP Injector | 47.3 | 64.7 | 51.3 | 32.7 | 29.5 | 32.1 | 33.9 |

Table 3. **Ablation studies on the components in SideFormer.** The combination of SAM extractor and CLIP injector shows the best performance.

| Strategy | COCO val | | LVIS MiniVal | |
|---------------------------|---------------------|--------------------|---------------------|--------------------|
| | AR _{@1000} | AP | AR _{@1000} | AP |
| Vanilla RPN [39] | 65.4 | 47.3 | 49.1 | 32.7 |
| Open-set RPN [#] | 67.5 (+2.1) | 46.7 (-0.6) | 54.8 (+5.7) | 29.3 (-3.4) |
| Open-set RPN | 67.5 (+2.1) | 48.6 (+1.3) | 54.8 (+5.7) | 33.1 (+0.4) |

Table 4. **Ablation studies on Open-set RPN.** Without further fine-tuning using additional region proposals from Open-set RPN (denoted as [#]), the improvement in proposal quality (AR_{@1000}) brought by Open-set RPN cannot be directly translated to an increase in detection performance (AP). Fine-tuning serves as a remedy for this discrepancy, yielding superior results.

| Proposal | AR _{@1000} | AP | AP ₅₀ | AP ₇₅ | AR _s | AP _m | AP _l |
|--------------|---------------------|-------------|------------------|------------------|-----------------|-----------------|-----------------|
| only RPN | 65.4 | 47.3 | 64.7 | 51.3 | 33.5 | 53.2 | 61.4 |
| only SAM | 59.4 | 46.8 | 63.3 | 51.1 | 29.8 | 52.2 | 65.0 |
| Open-set RPN | 67.5 | 48.6 | 66.1 | 52.7 | 33.5 | 53.2 | 64.2 |

Table 5. **Ablation studies on region proposal sources** for COCO 2017val. Using region proposals only from the SAM head exhibits a noticeable performance gap, particularly for small objects. The Open-set RPN effectively combines two sets of proposals, thereby achieving optimal performance.

domain gap exists between these and SAM features. Consequently, the inclusion of CLIP visual features can effectively bridge this gap and greatly benefit Sambor.

4.3.2 Effectiveness of Open-Set RPN

As elaborated in Sec. 3.3, the automatic mask generation pipeline of SAM allows for producing a number of high-quality open-set proposals, serving as a valuable complement to the vanilla RPN. We employ a 32×32 grid of points to generate open-set proposals, with a post-processing NMS threshold set to 0.7. Table 4 illustrates the average recall (AR_{@1000}) for region proposals. Notably, the inclusion of these open-set proposals results in a significant improvement in AR. However, the improved quality of region proposals does not manifest as superior detection performance; instead, there has been a decline. We posit that this is attributed to the detection head in the second stage not being exposed to the additional region proposals during training, thereby hindering its effective handling them.

To address this issue, we conduct a minor-scale fine-tuning adopting the Open-set RPN, *i.e.*, incorporating these open-set proposals during training. Specifically, with considerations for training efficiency, we employ a 32×32 grid of points to fine-tune for one epoch on approximately one-fifth of the O365 dataset. Maintaining all other hyperparameters constant, employing a reduced learning rate of 4×10^{-5} contributes to the efficacy of fine-tuning. It effectively eradicates inconsistencies in results, leading to superior performance for the Open-set RPN. Compared to the vanilla RPN, there is an improvement of 1.3 AP on COCO and 0.4 AP on LVIS. Unless specified otherwise, the Open-set RPN described elsewhere in this paper is fine-tuned.

Region proposal sources. After establishing the effectiveness of the Open-set RPN, a relevant question arises: *What would be the impact if we solely rely on region proposals from the SAM head?* We conduct ablation studies on the model fine-tuned with Open-set RPN. The evaluations include performance using proposals only from RPN, proposals only from the SAM head, and a combination of both sets, as shown in Table 5. Only RPN performance remains consistent compared to before fine-tuning (first row in Table 4). This confirms that the performance improvement in Open-set RPN is attributed to the supplementary proposals rather than the fine-tuning impact on RPN. When relying solely on proposals from the SAM head, to ensure an adequate quantity, we increase the density of grid points to 64×64 and set the NMS threshold to 0.95. There is a noticeable decrease in detection performance, especially for small objects. The difficulty of precisely targeting small objects with sampling points contributes to the inability to recall them, aligning with the results shown in [25]. Moreover, continuously increasing the density is impractical as it introduces unbearable computational and time consumption. Hence, the integration of the trainable RPN is crucial. The Open-set effectively combines the two sets of region proposals in a complementary fashion, achieving optimal performance.

4.4. Analyses

End-to-end open-vocabulary detector built upon SAM.

The release of SAM sparked significant interest within the community, giving rise to numerous derivative models based on it. One notable example is Grounded SAM [1], where the outputs from Grounding DINO are fed into SAM. This cascade transforms detection boxes for arbitrary objects into segmentation masks, achieving impressive visual effects. However, these efforts have remained at the level of simple connections between input and output interfaces of multiple models. In contrast, our Sambor goes beyond this by seamlessly integrating SAM and an open-vocabulary detector into an end-to-end framework. It not only achieves feature sharing but also facilitates the efficiency of interactive operations within the system.

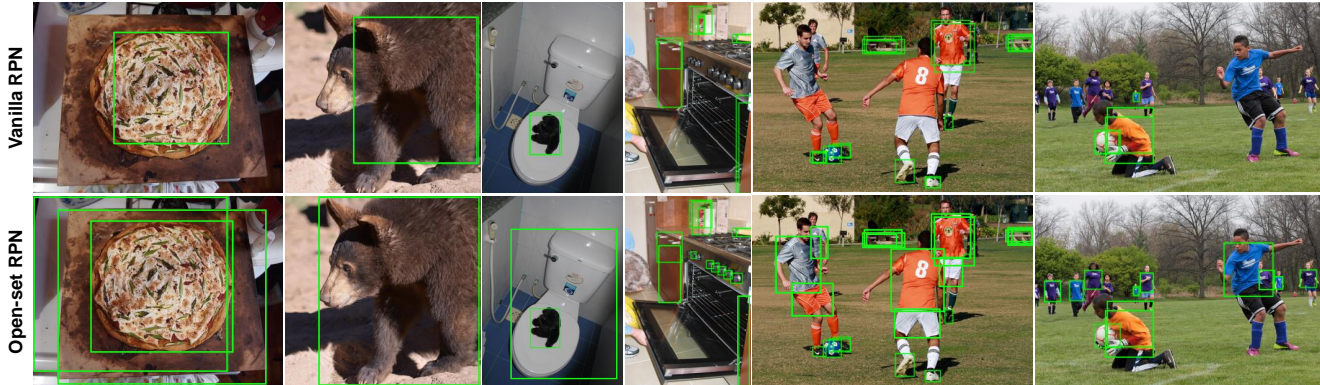


Figure 3. Visualization comparison between Open-set RPN and the vanilla RPN. For clarity, we only display high-quality region proposals with an IoU greater than 0.7 with ground truth. In the first two examples, the vanilla RPN fails to generate proposals meeting this criterion; thus, we show the one with the highest IoU.

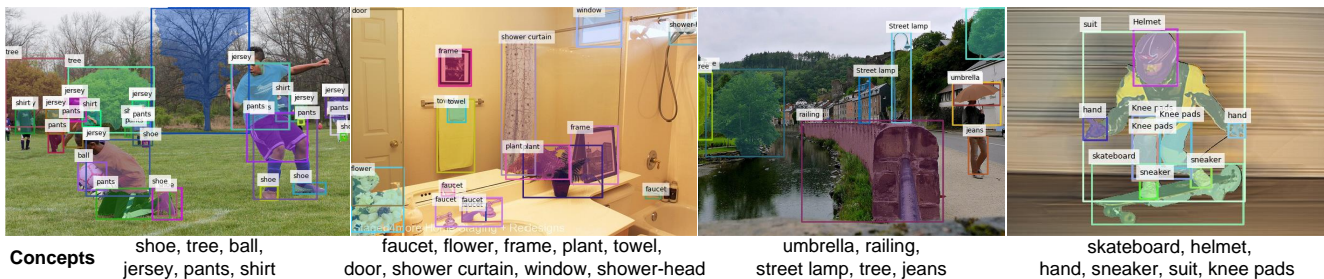


Figure 4. Visualization of Sambor for open-vocabulary detection. For better mask visual effects, we adopt the HQ-SAM [22] mask decoder.

Specifically, the strengths of Sambor manifest in the symbiotic integration of SAM with the open-vocabulary object detector, resulting in a mutually beneficial relationship. (1) SAM provides the detector with features possessing generalization capabilities, yielding competitive zero-shot transfer performance after semantic information supplementation. Moreover, the Open-set RPN leveraging region proposals generated by SAM further enhances the detection results. (2) The open-vocabulary object detector endows SAM to recognize arbitrary objects. Consequently, when utilizing certain functionalities of SAM, *e.g.*, interactive prompts, the detector can predict the categories while outputting segmentation results. This facilitates a more effortless and accurate acquisition of the desired targets.

Visualization of Open-set RPN. The comparison of region proposal results between Open-set RPN and the vanilla RPN is illustrated in Fig. 3. It is evident that, thanks to additional region proposals with robust zero-shot generalization, Open-set RPN effectively compensates for the recall of some objects, thereby addressing more challenging scenarios. For example, it can accurately capture the overall edges of an object and effectively leverage color information to delineate a person’s clothing, areas where the vanilla RPN performs inadequately.

Visualization of Sambor. We show the open-vocabulary detection results of Sambor in Fig. 4. The detection of desired category of objects is achieved by inputting concepts. Additionally, we feed the detection boxes into SAM head to obtain instance segmentation masks.

5. Conclusion

Sambor is an end-to-end open-vocabulary object detector that integrates the vision foundation model SAM. It effectively leverages the SAM features along with class-agnostic proposals to boost object detection. On the other hand, the open-vocabulary object detector supplements SAM with the lacking classification capability, thus empowering it to extend beyond segmenting anything to recognizing arbitrary categories. Experiments demonstrate superior open-vocabulary performance of Sambor and the contributions of the proposed module. We aim for this effort to be an effective attempt, equipping SAM with recognition capabilities to address a wider array of application needs, and offering a potential direction for open-vocabulary object detection.

Limitations. While Sambor demonstrates competitive performance in open-vocabulary object detection, it has yet to be scaled; for instance, by leveraging larger image-text

paired datasets for training to enhance its recognition capabilities in broad concepts. Additionally, the ability for few-shot learning plays a crucial role in expanding the functionality and applicability, with the potential for gradual improvement through integration with more interactive operations. We leave these refinements in future work.

Acknowledgment

This work is partially supported by the National Key R&D Program of China under Grant 2021ZD0112801.

A. More Results

Zero-shot instance segmentation on LVIS. We present the performance in Table 6, where the mask results are generated by prompting the detection boxes (shown in Table 2) to the SAM head. Compared to X-Decoder [67] and OpenSeeD [58], our Sambor exhibits superior performance, indicating its robust zero-shot generalization capabilities.

More visualization results. Fig. 5 and 6 provide more qualitative visualization results with open-vocabulary concepts, using images from LVIS MiniVal. We leverage the HQ-SAM [22] mask decoder to showcase superior segmentation outcomes. Without the need for additional training, the modules employed for mask generation can be seamlessly integrated into Sambor.

B. More Implementation Details

Pre-training details. Table 7 summarizes the detailed settings we use for pre-training and fine-tuning. In addition, for the Cascade R-CNN [3] detector head, we employ a modified Focal Loss [30] (adapted in the form of word-region alignment) for classification, and the SmoothL1 Loss [13] is implemented for regression.

Open-set RPN. Based on region proposals obtained from RPN, we augment with additional high-quality proposals from the SAM head. Leveraging the automatic mask generation pipeline in SAM, we obtain proposals using a 32×32 grid of points, with the IoU prediction serving as the score. However, due to a domain gap in the prediction scores between the proposals in the two sets, directly merging them is not reasonable. Therefore, our approach involves selecting the top 1,000 proposals from RPN and conducting an initial screening through NMS with a threshold of 0.7. Subsequently, we regard the scores of the retained proposals as 1.0 and merge them with additional proposals from the SAM head. Finally, we employ another round of NMS (with the same threshold of 0.7) to filter out highly overlapping proposals, obtaining a maximum of 1,000 proposals as the output of the Open-set RPN.

Text prompts. Since the vision-language foundation model is trained with complete sentences, we input the concepts

| Method | Pre-Train Data | MiniVal | | | | Val 1.0 |
|----------------------------|-----------------------|-------------|-----------------|-----------------|-----------------|-------------|
| | | AP | AP _r | AP _c | AP _f | AP |
| X-Decoder (T) [67] | COCO,C4M [†] | - | - | - | - | 9.6 |
| OpenSeeD (T) [58] | O365,COCO | - | - | - | - | 19.4 |
| OpenSeeD (L) [58] | O365,COCO | - | - | - | - | 21.0 |
| Sambor [★] (Ours) | O365 | 27.6 | 27.3 | 27.5 | 27.7 | 21.7 |
| Sambor [★] (Ours) | O365,GoldG | 35.7 | 31.4 | 37.1 | 35.3 | 29.4 |

Table 6. **Zero-shot instance segmentation performance** on LVIS benchmark. *Fixed* AP [8] is reported. AP_r, AP_c, and AP_f indicate the AP values for rare, common and frequent categories, respectively. [†] includes Conceptual Captions [41], SBU Captions [46], Visual Genome [26], and COCO Captions [5]. [★] denotes the application of Open-set RPN.

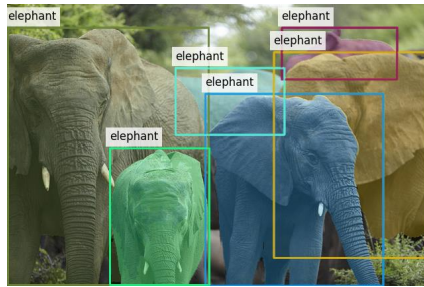
| Configuration | Value |
|----------------------------------|--------------------------|
| Pre-training: | |
| Dataset | O365 |
| SAM Backbone | ViT-B |
| CLIP Backbone | RN50×64 |
| Training Epochs | 12 |
| Batch Size | 64 |
| Optimizer | AdamW |
| LR | 4×10^{-4} |
| LR Schedule | CosineAnnealing |
| Weight Decay | 0.05 |
| Warmup Iters | 1,000 |
| Image Resolution | 1,024×1,024 |
| Augmentation | Random Flip, SSJ [12] |
| Max Text Token Length | 77 |
| SideFormer Attention | DeformableAttention [66] |
| # of Attention Heads | 8 |
| Feedforward Channels | 3072 |
| Open-set RPN Fine-tuning: | |
| Dataset | $\approx 1/5$ O365 |
| LR | 4×10^{-5} |
| Training Epochs | 1 |
| # of Grid Points | 32×32 |
| RPN NMS Threshold | 0.7 |
| Unified Data Fine-tuning: | |
| Dataset | O365 + GoldG |
| LR | 4×10^{-4} |
| Training Epochs | 3 |
| # of Concepts [†] | 150 |

Table 7. **Detailed training settings** of Sambor. [†] denotes only for phrase grounding data.

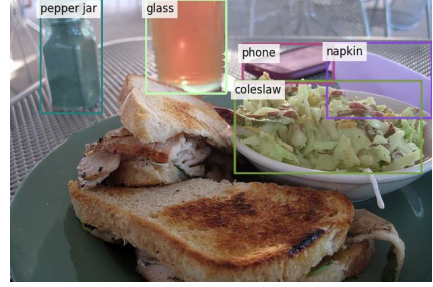
into a prompt template and use an ensemble of diverse prompts. We utilize a list of 80 prompt templates following [38] without bells and whistles.



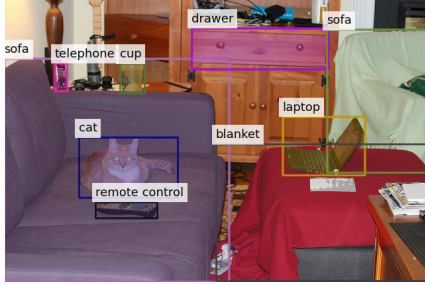
refrigerator, range hood, stove, dishtowel, paper towel, bowl, dishwasher, microwave



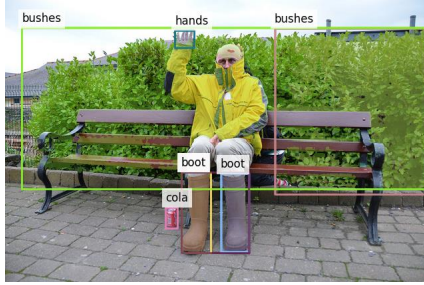
elephant



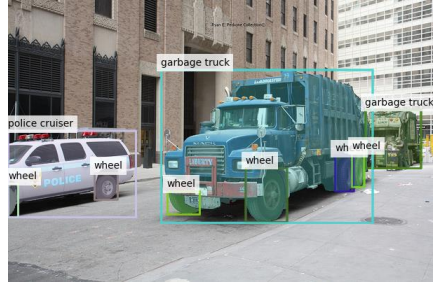
pepper jar, phone, napkin, coleslaw, glass



sofa, cat, remote control, blanket, laptop, telephone, cup, drawer



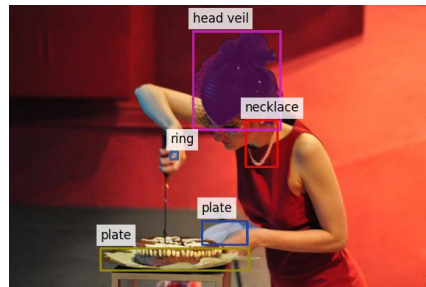
bushes, hands, boot, cola



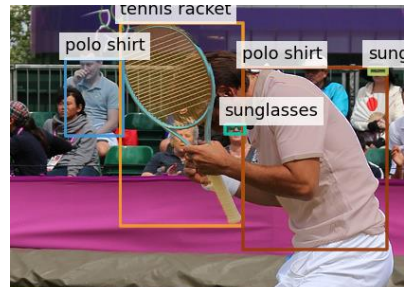
garbage truck, wheel, police cruiser



knob, tray, refrigerator, toaster



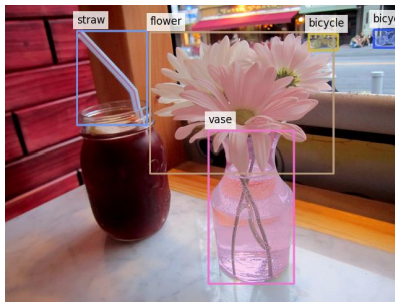
plate, necklace, head veil, ring



tennis racket, polo shirt, sunglasses



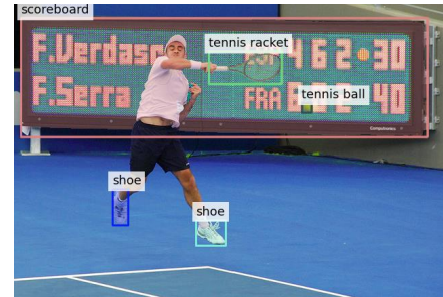
helmet, belt, folding chair, baseball bat, home plate (baseball), knee pad, baseball glove



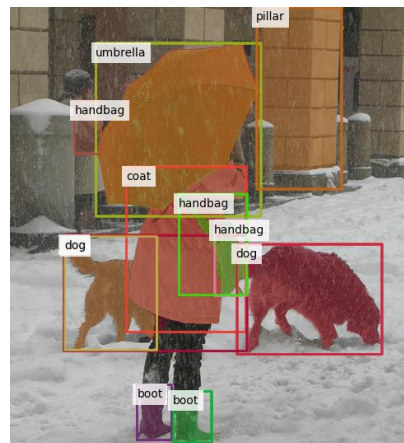
vase, straw, bicycle, flower



sea, umbrella, deck chair, towel



tennis racket, tennis ball, shoe, scoreboard



umbrella, handbag, dog, boot, pillar

Figure 5. Qualitative results of Sambor with open-vocabulary concepts showcased.

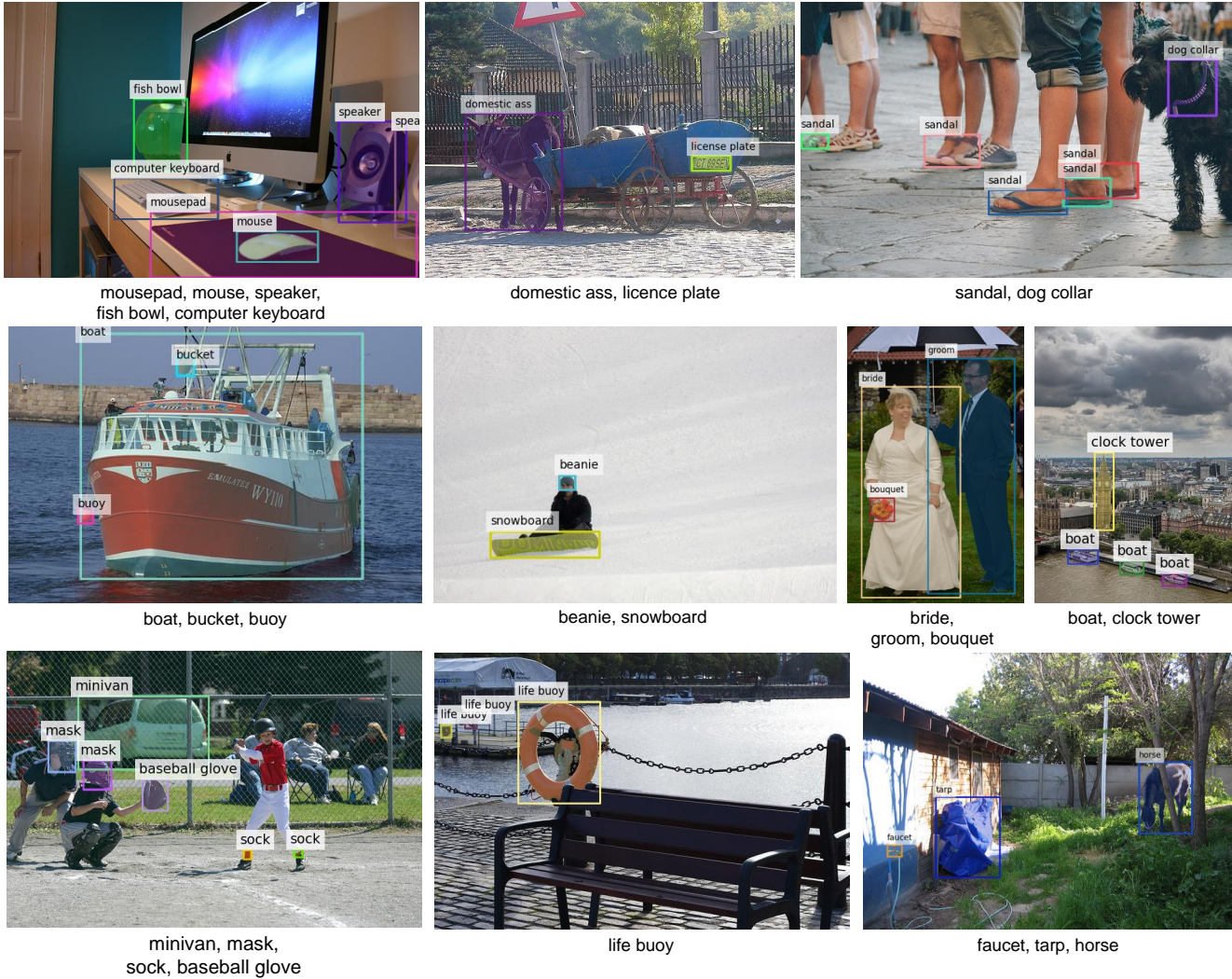


Figure 6. Qualitative results of Sambor with open-vocabulary concepts showcased.

References

- [1] Grounded segment anything. <https://github.com/IDEA-Research/Grounded-Segment-Anything>, 2023. 1, 2, 7
- [2] Jimmy Lei Ba, Jamie Ryan Kiros, and Geoffrey E Hinton. Layer normalization. *arXiv preprint arXiv:1607.06450*, 2016. 4
- [3] Zhaowei Cai and Nuno Vasconcelos. Cascade r-cnn: Delving into high quality object detection. In *CVPR*, pages 6154–6162, 2018. 3, 4, 6, 9
- [4] Kai Chen, Jiaqi Wang, Jiangmiao Pang, Yuhang Cao, Yu Xiong, Xiaoxiao Li, Shuyang Sun, Wansheng Feng, Ziwei Liu, Jiarui Xu, Zheng Zhang, Dazhi Cheng, Chenchen Zhu, Tianheng Cheng, Qijie Zhao, Buyu Li, Xin Lu, Rui Zhu, Yue Wu, Jifeng Dai, Jingdong Wang, Jianping Shi, Wanli Ouyang, Chen Change Loy, and Dahua Lin. MMDetection: Open mmlab detection toolbox and benchmark. *arXiv preprint arXiv:1906.07155*, 2019. 5
- [5] Xinlei Chen, Hao Fang, Tsung-Yi Lin, Ramakrishna Vedantam, Saurabh Gupta, Piotr Dollár, and C. Lawrence Zitnick. Microsoft COCO captions: Data collection and evaluation server. *arXiv preprint arXiv:1504.00325*, 2015. 9
- [6] Zhe Chen, Yuchen Duan, Wenhui Wang, Junjun He, Tong Lu, Jifeng Dai, and Yu Qiao. Vision transformer adapter for dense predictions. *arXiv preprint arXiv:2205.08534*, 2022. 2, 3
- [7] Xiyang Dai, Yinpeng Chen, Bin Xiao, Dongdong Chen, Mengchen Liu, Lu Yuan, and Lei Zhang. Dynamic head: Unifying object detection heads with attentions. In *CVPR*, pages 7373–7382, 2021. 5
- [8] Achal Dave, Piotr Dollár, Deva Ramanan, Alexander Kirillov, and Ross B. Girshick. Evaluating large-vocabulary object detectors: The devil is in the details. *arXiv preprint arXiv:2102.01066*, 2021. 6, 9
- [9] Alexey Dosovitskiy, Lucas Beyer, Alexander Kolesnikov, Dirk Weissenborn, Xiaohua Zhai, Thomas Unterthiner, Mostafa Dehghani, Matthias Minderer, Georg Heigold, Syl-

- vain Gelly, et al. An image is worth 16x16 words: Transformers for image recognition at scale. *arXiv preprint arXiv:2010.11929*, 2020. 3, 4, 5, 6
- [10] Yu Du, Fangyun Wei, Zihe Zhang, Miaoqing Shi, Yue Gao, and Guoqi Li. Learning to prompt for open-vocabulary object detection with vision-language model. In *CVPR*, pages 14084–14093, 2022. 1, 2
- [11] Peng Gao, Shijie Geng, Renrui Zhang, Teli Ma, Rongyao Fang, Yongfeng Zhang, Hongsheng Li, and Yu Qiao. Clip-adapter: Better vision-language models with feature adapters. *IJCV*, pages 1–15, 2023. 2
- [12] Golnaz Ghiasi, Yin Cui, Aravind Srinivas, Rui Qian, Tsung-Yi Lin, Ekin D. Cubuk, Quoc V. Le, and Barret Zoph. Simple copy-paste is a strong data augmentation method for instance segmentation. In *CVPR*, 2021. 5, 9
- [13] Ross Girshick. Fast r-cnn. In *ICCV*, pages 1440–1448, 2015. 9
- [14] Xiuye Gu, Tsung-Yi Lin, Weicheng Kuo, and Yin Cui. Open-vocabulary object detection via vision and language knowledge distillation. *arXiv preprint arXiv:2104.13921*, 2021. 1, 2
- [15] Agrim Gupta, Piotr Dollar, and Ross Girshick. Lvis: A dataset for large vocabulary instance segmentation. In *CVPR*, pages 5356–5364, 2019. 2, 6
- [16] Kaiming He, Xiangyu Zhang, Shaoqing Ren, and Jian Sun. Deep residual learning for image recognition. In *CVPR*, pages 770–778, 2016. 3, 5, 6
- [17] Kaiming He, Georgia Gkioxari, Piotr Dollár, and Ross Girshick. Mask r-cnn. In *ICCV*, pages 2961–2969, 2017. 3
- [18] Kaiming He, Xinlei Chen, Saining Xie, Yanghao Li, Piotr Dollár, and Ross B. Girshick. Masked autoencoders are scalable vision learners. In *CVPR*, pages 15979–15988, 2022. 1
- [19] Drew A Hudson and Christopher D Manning. Gqa: A new dataset for real-world visual reasoning and compositional question answering. In *CVPR*, pages 6700–6709, 2019. 5
- [20] Chao Jia, Yinfei Yang, Ye Xia, Yi-Ting Chen, Zarana Parekh, Hieu Pham, Quoc Le, Yun-Hsuan Sung, Zhen Li, and Tom Duerig. Scaling up visual and vision-language representation learning with noisy text supervision. In *ICML*, pages 4904–4916. PMLR, 2021. 1, 2
- [21] Aishwarya Kamath, Mannat Singh, Yann LeCun, Gabriel Synnaeve, Ishan Misra, and Nicolas Carion. Mdetr-modulated detection for end-to-end multi-modal understanding. In *ICCV*, pages 1780–1790, 2021. 5, 6
- [22] Lei Ke, Mingqiao Ye, Martin Danelljan, Yifan Liu, Yu-Wing Tai, Chi-Keung Tang, and Fisher Yu. Segment anything in high quality. *arXiv preprint arXiv:2306.01567*, 2023. 2, 8, 9
- [23] Muhammad Uzair Khattak, Hanoona Rasheed, Muhammad Maaz, Salman Khan, and Fahad Shahbaz Khan. Maple: Multi-modal prompt learning. In *CVPR*, pages 19113–19122, 2023. 2
- [24] Diederik P. Kingma and Jimmy Ba. Adam: A method for stochastic optimization. In *ICLR*, 2015. 5
- [25] Alexander Kirillov, Eric Mintun, Nikhila Ravi, Hanzi Mao, Chloe Rolland, Laura Gustafson, Tete Xiao, Spencer Whitehead, Alexander C. Berg, Wan-Yen Lo, Piotr Dollár, and Ross Girshick. Segment anything. *arXiv preprint arXiv:2304.02643*, 2023. 1, 2, 3, 4, 5, 7
- [26] Ranjay Krishna, Yuke Zhu, Oliver Groth, Justin Johnson, Kenji Hata, Joshua Kravitz, Stephanie Chen, Yannis Kalantidis, Li-Jia Li, David A Shamma, et al. Visual genome: Connecting language and vision using crowdsourced dense image annotations. *IJCV*, 123:32–73, 2017. 5, 9
- [27] Weicheng Kuo, Yin Cui, Xiuye Gu, AJ Piergiovanni, and Anelia Angelova. Open-vocabulary object detection upon frozen vision and language models. In *ICLR*, 2023. 1, 2, 3
- [28] Liunian Harold Li, Pengchuan Zhang, Haotian Zhang, Jianwei Yang, Chunyuan Li, Yiwu Zhong, Lijuan Wang, Lu Yuan, Lei Zhang, Jenq-Neng Hwang, et al. Grounded language-image pre-training. In *CVPR*, pages 10965–10975, 2022. 1, 2, 3, 4, 5, 6
- [29] Yanghao Li, Hanzi Mao, Ross Girshick, and Kaiming He. Exploring plain vision transformer backbones for object detection. In *ECCV*, pages 280–296, 2022. 3, 4, 5
- [30] Tsung-Yi Lin, Priya Goyal, Ross B. Girshick, Kaiming He, and Piotr Dollár. Focal loss for dense object detection. In *ICCV*, 2017. 9
- [31] Tsung-Yi Lin, Michael Maire, Serge Belongie, James Hays, Pietro Perona, Deva Ramanan, Piotr Dollár, and C Lawrence Zitnick. Microsoft coco: Common objects in context. In *ECCV*, 2014. 2, 5
- [32] Shilong Liu, Zhaoyang Zeng, Tianhe Ren, Feng Li, Hao Zhang, Jie Yang, Chunyuan Li, Jianwei Yang, Hang Su, Jun Zhu, et al. Grounding dino: Marrying dino with grounded pre-training for open-set object detection. *arXiv preprint arXiv:2303.05499*, 2023. 1, 2, 3, 5, 6
- [33] Ze Liu, Yutong Lin, Yue Cao, Han Hu, Yixuan Wei, Zheng Zhang, Stephen Lin, and Baining Guo. Swin transformer: Hierarchical vision transformer using shifted windows. In *ICCV*, pages 10012–10022, 2021. 5, 6
- [34] Chuofan Ma, Yi Jiang, Xin Wen, Zehuan Yuan, and Xiaojuan Qi. Codet: Co-occurrence guided region-word alignment for open-vocabulary object detection. *arXiv preprint arXiv:2310.16667*, 2023. 2
- [35] Matthias Minderer, Alexey Gritsenko, Austin Stone, Maxim Neumann, Dirk Weissenborn, Alexey Dosovitskiy, Aravindh Mahendran, Anurag Arnab, Mostafa Dehghani, Zhuoran Shen, Xiao Wang, Xiaohua Zhai, Thomas Kipf, and Neil Houlsby. Simple open-vocabulary object detection with vision transformers. In *ECCV*, 2022. 1, 2
- [36] Maxime Oquab, Timothée Darcet, Theo Moutakanni, Huy V. Vo, Marc Szafraniec, Vasil Khalidov, Pierre Fernandez, Daniel Haziza, Francisco Massa, Alaaeldin El-Nouby, Russell Howes, Po-Yao Huang, Hu Xu, Vasu Sharma, Shang-Wen Li, Wojciech Galuba, Mike Rabbat, Mido Assran, Nicolas Ballas, Gabriel Synnaeve, Ishan Misra, Herve Jegou, Julien Mairal, Patrick Labatut, Armand Joulin, and Piotr Bojanowski. Dinov2: Learning robust visual features without supervision. *arXiv preprint arXiv:2304.07193*, 2023. 1
- [37] Bryan A Plummer, Liwei Wang, Chris M Cervantes, Juan C Caicedo, Julia Hockenmaier, and Svetlana Lazebnik. Flickr30k entities: Collecting region-to-phrase correspondences for richer image-to-sentence models. In *ICCV*, pages 2641–2649, 2015. 5
- [38] Alec Radford, Jong Wook Kim, Chris Hallacy, Aditya Ramesh, Gabriel Goh, Sandhini Agarwal, Girish Sastry,

- Amanda Askell, Pamela Mishkin, Jack Clark, et al. Learning transferable visual models from natural language supervision. In *ICML*, pages 8748–8763, 2021. 1, 2, 3, 4, 5, 9
- [39] Shaoqing Ren, Kaiming He, Ross Girshick, and Jian Sun. Faster r-cnn: Towards real-time object detection with region proposal networks. In *NeurIPS*, 2015. 2, 4, 7
- [40] Shuai Shao, Zeming Li, Tianyuan Zhang, Chao Peng, Gang Yu, Xiangyu Zhang, Jing Li, and Jian Sun. Objects365: A large-scale, high-quality dataset for object detection. In *ICCV*, pages 8430–8439, 2019. 5
- [41] Piyush Sharma, Nan Ding, Sebastian Goodman, and Radu Soricut. Conceptual captions: A cleaned, hypemymed, image alt-text dataset for automatic image captioning. In *ACL*, pages 2556–2565, 2018. 1, 9
- [42] Yi-Lin Sung, Jaemin Cho, and Mohit Bansal. Lst: Ladder side-tuning for parameter and memory efficient transfer learning. In *NeurIPS*, pages 12991–13005, 2022. 2, 3
- [43] Yi-Lin Sung, Jaemin Cho, and Mohit Bansal. VI-adapter: Parameter-efficient transfer learning for vision-and-language tasks. In *CVPR*, pages 5227–5237, 2022. 2
- [44] Bart Thomee, David A Shamma, Gerald Friedland, Benjamin Elizalde, Karl Ni, Douglas Poland, Damian Borth, and Li-Jia Li. Yfcc100m: The new data in multimedia research. *Communications of the ACM*, 59(2):64–73, 2016. 1
- [45] Ashish Vaswani, Noam Shazeer, Niki Parmar, Jakob Uszkoreit, Llion Jones, Aidan N Gomez, Łukasz Kaiser, and Illia Polosukhin. Attention is all you need. In *NeurIPS*, 2017. 4
- [46] Tomás F Yago Vicente, Le Hou, Chen-Ping Yu, Minh Hoai, and Dimitris Samaras. Large-scale training of shadow detectors with noisily-annotated shadow examples. In *ECCV*, pages 816–832, 2016. 1, 9
- [47] Teng Wang, Jinrui Zhang, Junjie Fei, Hao Zheng, Yunlong Tang, Zhe Li, Mingqi Gao, and Shanshan Zhao. Caption anything: Interactive image description with diverse multi-modal controls. *arXiv preprint arXiv:2305.02677*, 2023. 1
- [48] Size Wu, Wenwei Zhang, Sheng Jin, Wentao Liu, and Chen Change Loy. Aligning bag of regions for open-vocabulary object detection. In *CVPR*, 2023. 2
- [49] Xiaoshi Wu, Feng Zhu, Rui Zhao, and Hongsheng Li. Cora: Adapting clip for open-vocabulary detection with region prompting and anchor pre-matching. In *CVPR*, 2023. 2
- [50] Yifan Xu, Mengdan Zhang, Chaoyou Fu, Peixian Chen, Xiaoshan Yang, Ke Li, and Changsheng Xu. Multi-modal queried object detection in the wild. *arXiv preprint arXiv:2305.18980*, 2023. 2
- [51] Hantao Yao, Rui Zhang, and Changsheng Xu. Visual-language prompt tuning with knowledge-guided context optimization. In *CVPR*, pages 6757–6767, 2023. 2
- [52] Lewei Yao, Jianhua Han, Youpeng Wen, Xiaodan Liang, Dan Xu, Wei Zhang, Zhenguo Li, Chunjing Xu, and Hang Xu. Detclip: Dictionary-enriched visual-concept paralleled pre-training for open-world detection. In *NeurIPS*, pages 9125–9138, 2022. 1, 2, 4, 6
- [53] Lewei Yao, Jianhua Han, Xiaodan Liang, Dan Xu, Wei Zhang, Zhenguo Li, and Hang Xu. Detclipv2: Scalable open-vocabulary object detection pre-training via word-region alignment. In *CVPR*, 2023. 2, 4, 6
- [54] Yuhang Zang, Wei Li, Kaiyang Zhou, Chen Huang, and Chen Change Loy. Open-vocabulary detr with conditional matching. In *ECCV*, 2022.
- [55] Alireza Zareian, Kevin Dela Rosa, Derek Hao Hu, and Shih-Fu Chang. Open-vocabulary object detection using captions. In *CVPR*, pages 14393–14402, 2021. 2
- [56] H Zhang, F Li, S Liu, L Zhang, H Su, J Zhu, LM Ni, and HY Shum. Dino: Detr with improved denoising anchor boxes for end-to-end object detection. arxiv 2022. *arXiv preprint arXiv:2203.03605*, 2022. 5
- [57] Haotian Zhang, Pengchuan Zhang, Xiaowei Hu, Yen-Chun Chen, Liunian Li, Xiyang Dai, Lijuan Wang, Lu Yuan, Jenq-Neng Hwang, and Jianfeng Gao. Glipv2: Unifying localization and vision-language understanding. In *NeurIPS*, pages 36067–36080, 2022. 6
- [58] Hao Zhang, Feng Li, Xueyan Zou, Shilong Liu, Chunyuan Li, Jianwei Yang, and Lei Zhang. A simple framework for open-vocabulary segmentation and detection. In *ICCV*, pages 1020–1031, 2023. 2, 9
- [59] Jeffrey O Zhang, Alexander Sax, Amir Zamir, Leonidas Guibas, and Jitendra Malik. Side-tuning: a baseline for network adaptation via additive side networks. In *ECCV*, pages 698–714, 2020. 2
- [60] Renrui Zhang, Rongyao Fang, Wei Zhang, Peng Gao, Kunchang Li, Jifeng Dai, Yu Qiao, and Hongsheng Li. Tip-adapter: Training-free clip-adapter for better vision-language modeling. *arXiv preprint arXiv:2111.03930*, 2021. 2
- [61] Yuanhan Zhang, Qinghong Sun, Yichun Zhou, Zexin He, Zhenfei Yin, Kun Wang, Lu Sheng, Yu Qiao, Jing Shao, and Ziwei Liu. Bamboo: Building mega-scale vision dataset continually with human-machine synergy. *arXiv preprint arXiv:2203.07845*, 2022. 5
- [62] Yiwu Zhong, Jianwei Yang, Pengchuan Zhang, Chunyuan Li, Noel Codella, Liunian Harold Li, Luwei Zhou, Xiyang Dai, Lu Yuan, Yin Li, et al. Regionclip: Region-based language-image pretraining. In *CVPR*, 2022. 1, 2
- [63] Kaiyang Zhou, Jingkang Yang, Chen Change Loy, and Ziwei Liu. Conditional prompt learning for vision-language models. In *CVPR*, pages 16816–16825, 2022. 2
- [64] Kaiyang Zhou, Jingkang Yang, Chen Change Loy, and Ziwei Liu. Learning to prompt for vision-language models. *IJCV*, 130(9):2337–2348, 2022. 2
- [65] Xingyi Zhou, Rohit Girdhar, Armand Joulin, Philipp Krähenbühl, and Ishan Misra. Detecting twenty-thousand classes using image-level supervision. In *ECCV*, 2022. 2
- [66] Xizhou Zhu, Weijie Su, Lewei Lu, Bin Li, Xiaogang Wang, and Jifeng Dai. Deformable DETR: deformable transformers for end-to-end object detection. In *ICLR*, 2021. 9
- [67] Xueyan Zou, Zi-Yi Dou, Jianwei Yang, Zhe Gan, Linjie Li, Chunyuan Li, Xiyang Dai, Harkirat Behl, Jianfeng Wang, Lu Yuan, Nanyun Peng, Lijuan Wang, Yong Jae Lee, and Jianfeng Gao. Generalized decoding for pixel, image, and language. In *CVPR*, pages 15116–15127, 2023. 2, 9
- [68] Xueyan Zou, Jianwei Yang, Hao Zhang, Feng Li, Linjie Li, Jianfeng Gao, and Yong Jae Lee. Segment everything everywhere all at once. *arXiv preprint arXiv:2304.06718*, 2023. 2